HAL
archives-ouvertes.fr

Electrochemical activity of various types of aqueous In(III) species at a mercury electrode

Raewyn Town, Jérôme Duval, Herman van Leeuwen

▶ **To cite this version:**

Raewyn Town, Jérôme Duval, Herman van Leeuwen. Electrochemical activity of various types of aqueous In(III) species at a mercury electrode. Journal of Solid State Electrochemistry, Springer Verlag, 2020, 10.1007/s10008-020-04607-0 . hal-02941348

HAL Id: hal-02941348
https://hal.univ-lorraine.fr/hal-02941348

Submitted on 24 Sep 2020

HAL is a multi-disciplinary open access archive for the deposit and dissemination of scientific research documents, whether they are published or not. The documents may come from teaching and research institutions in France or abroad, or from public or private research centers.

L'archive ouverte pluridisciplinaire **HAL**, est destinée au dépôt et à la diffusion de documents scientifiques de niveau recherche, publiés ou non, émanant des établissements d'enseignement et de recherche français ou étrangers, des laboratoires publics ou privés.

Journal of Solid State Electrochemistry

Electrochemical activity of various types of aqueous In(III) species at a mercury electrode

--Manuscript Draft--

Manuscript Number:	JSEL-D-20-00228R1
Full Title:	Electrochemical activity of various types of aqueous In(III) species at a mercury electrode
Article Type:	Original Paper
Corresponding Author:	Raewyn Town Universiteit Antwerpen Antwerpen, BELGIUM
Corresponding Author Secondary Information:	
Corresponding Author's Institution:	Universiteit Antwerpen
Corresponding Author's Secondary Institution:	
First Author:	Raewyn M. Town
First Author Secondary Information:	
Order of Authors:	Raewyn M. Town
	Jérôme Duval
	Herman P. van Leeuwen
Order of Authors Secondary Information:	
Abstract:	An interpretation framework is presented which provides a straightforward means to characterise the electrochemical reactivity of aqueous ions together with their various hydrolysed counterparts. Our novel approach bypasses the more laborious strategy of solving rigorously, for all relevant species, the complete set of Butler Volmer equations coupled to diffusion differential equations. Specifically we consider the spatial variable via a Koutecky-Koryta type of differentiation between nonlabile and labile zones adjacent to the electrode. The theory is illustrated by an assessment of the electrochemical reactivity of aqueous In(III) species based upon proper comparison between relevant time scales of the involved interfacial processes, i.e. diffusion, (de)protonation of inner-sphere water, dissociation/release of H 2 O and OH - , and electron transfer. The analysis reveals that whilst all In(III) species are labile on the experimental timescale with respect to (de)protonation and (de)hydration, there are large differences in the rates of electron transfer between In(H 2 O) 6 3+ and the various hydroxy species. Specifically, in the case of In(H 2 O) 6 3+ the rate of electron transfer is so slow that it replaces the traditional Eigen rate-limiting water release step in the overall passage from hydrated In 3+ to its reduced metallic form; in contrast the In(III) hydroxy species display electrochemically reversible behaviour.

Powered by Editorial Manager® and ProduXion Manager® from Aries Systems Corporation

Electrochemical activity of various types of aqueous In(III) species at a mercury electrode

Raewyn M. Town[a,b*], Jérôme F. L. Duval[c], and Herman P. van Leeuwen[b]

[a] Systemic Physiological and Ecotoxicological Research (SPHERE), Department of Biology, Universiteit Antwerpen, Groenenborgerlaan 171, 2020 Antwerpen, Belgium. Corresponding author: raewyn.town@uantwerpen.be

[b] Physical Chemistry and Soft Matter, Wageningen University & Research, Stippeneng 4, 6708 WE Wageningen, The Netherlands

[c] Université de Lorraine, CNRS, Laboratoire Interdisciplinaire des Environnements Continentaux (LIEC), F-54000 Nancy, France

Abstract

An interpretation framework is presented which provides a straightforward means to characterise the electrochemical reactivity of aqueous ions together with their various hydrolysed counterparts. Our novel approach bypasses the more laborious strategy of solving rigorously, for all relevant species, the complete set of Butler Volmer equations coupled to diffusion differential equations. Specifically we consider the spatial variable via a Koutecky-Koryta type of differentiation between nonlabile and labile zones adjacent to the electrode. The theory is illustrated by an assessment of the electrochemical reactivity of aqueous In(III) species based upon proper comparison between relevant time scales of the involved interfacial processes, i.e. diffusion, (de)protonation of inner-sphere water, dissociation/release of H_2O and OH^-, and electron transfer. The analysis reveals that whilst all In(III) species are labile on the experimental timescale with respect to (de)protonation and (de)hydration, there are large differences in the rates of electron transfer between $In(H_2O)_6^{3+}$ and the various hydroxy species. Specifically, in the case of $In(H_2O)_6^{3+}$ the rate of electron transfer is so slow that it replaces the traditional Eigen rate-limiting water release step in the overall passage from hydrated In^{3+} to its reduced metallic form; in contrast the In(III) hydroxy species display electrochemically reversible behaviour.

Keywords electrochemical irreversibility, indium, SSCP, reaction layer, lability

Declarations

Funding: RMT conducted this research within the EnviroStress and EXPOSOME centers of excellence funded by Universiteit Antwerpen's Bijzonder Onderzoeksfonds (BOF).

Conflicts of interest: The authors declare that they have no conflict of interest.

Availability of data and material: All data analysed during this study are included in this manuscript.

Code availability: Not applicable.

Introduction

The electrochemical features of In(III) in aqueous solution are strongly pH-dependent. In(III) readily hydrolyses at low pH: see ref [1] for a critical review of the literature on the hydrolysis constants. Literature from the 1960s evidences that voltammetric waves recorded for free $In(H_2O)_6^{3+}$ with a dropping mercury electrode at a pH sufficiently low to suppress hydrolysis, show a drawn-out electrochemically irreversible wave for the $In(H_2O)_6^{3+}$ species with halfwave potential, $E_{1/2}$, of -0.95 V (*vs.* saturated calomel electrode (SCE)); as the pH is increased an electrochemically reversible diffusion-controlled wave with $E_{1/2}$ of -0.55 V (*vs.* SCE) is observed [2-4]. These observations suggest that In(III) hydroxy species are the predominant electroactive contributors to the electrodic reduction current [5-7].

In recent years, the widespread use of so-called technology relevant elements such as indium will potentially lead to increasing concentrations of such elements in the environment [8]. This situation has motivated efforts to apply electroanalytical techniques to the determination of In(III) species in aqueous media. Some of these have made the assumption that $In(H_2O)_6^{3+}$ is the exclusively measured species [9-11], which at first sight seems questionable in light of its established electrochemical irreversibility.

The potential for increasing amounts of In(III) to be released into the environment also calls for evaluation of its bioavailability and potential ecotoxicological effects [12-15]. In the case of algae, the concentration of the $In(H_2O)_6^{3+}$ species was shown to be a poor predictor of biouptake [16]. A proper understanding of the (electro)chemical reactivity of In(III) is fundamental to characterising and predicting its bioavailability and potential toxicity [17].

A rigorous analysis of the overall In(III) reduction process in aqueous media requires consideration of the electrochemical activity of the various trivalent In species. The overall electrochemical activity derives from the rates of electron transfer of each species (electrochemical reversibility), the rates of dehydration or even mere deprotonation of H_2O in the inner-hydration sphere of each ion, as well as the lability of each species on the effective timescale of the measuring methodology. For example, the reported greater electrochemical reactivity of In(III) hydroxy species goes in hand with their enhanced dehydration rates as compared to that of the aqueous ion $In(H_2O)_6^{3+}$ [18]. Similarly, the ability of coordinated halides to facilitate In(III) electroreduction is ascribed to their labilizing effect on the remaining inner-sphere water molecules [4, 19-21]. The pH dependent features of the voltammetric waves for In(III) further suggest that the irreversibility of $In(H_2O)_6^{3+}$ reduction by a mercury electrode is so strong that its rate of dehydration is fast compared to that for electron transfer. Herein we develop a conceptual framework to describe the electrochemical reactivity and chemodynamic features of aqueous In(III) species. The treatment includes accounting for their rates of electron transfer together with their rates of formation and dissociation. The theoretical concepts are

successfully illustrated by experimental data obtained by stripping chronopotentiometry at scanned deposition potential (SSCP) [22-24].

Theory

In the bulk aqueous medium, the very fast exchange rate of protons warrants true equilibrium to be established between the various types of In(III) species (see Table 1 and elaboration below). Thus, maintenance of equilibrium over a steady-state diffusion layer adjacent to the interface between a macroelectrode and the aqueous medium is also expected (see below). Differences in reactivity of the In(III) species, according to their pertaining relative rates of electron transfer, dehydration and/or (de)protonation, will show up in the reaction layer, i.e. the zone adjacent to the electrode/medium interface within which equilibrium is no longer maintained between the electroactive and electroinactive forms of the various In(III) species. In *all* these types of elementary processes, any In(III) species with a significant reactivity in *all* of them is inherently electroactive.

Reaction layer and lability considerations for the aqueous In(III) system

Computation of the reaction layer thickness during electrodic reduction of In(III) and ensuing analysis of the lability characteristics of the various In(III) species requires knowledge of the thermodynamic and kinetic features of their complexes with H_2O. In aqueous solution, In(III) has 6 water molecules in its inner-hydration sphere [25, 26]. To our knowledge, there are no reliable published data on the dehydration rate constants, k_w, for In(III) species [27]; for $In(H_2O)_6^{3+}$ a tentative value for k_w of the order of 100 s^{-1} has been indicated [28]. As a proxy, we proceed using the k_w values reported for Fe(III) species as a kind of guide, i.e.: $k_w(Fe(H_2O)_6^{3+}) = 200\ s^{-1}$; $k_w(Fe(H_2O)_5OH^{2+}) = 10^5\ s^{-1}$; $k_w(Fe(H_2O)_4(OH)_2^{+} = 10^7\ s^{-1}$; $k_w(Fe(H_2O)_3(OH)_3^{0} = 10^9\ s^{-1}$ [18]. In support of this approximation, we note that the k_w for Fe^{3+} is of the same order of magnitude as that reported for Ga^{3+} which is in the same periodic group as In [18]. These k_w values correspond to the dissociation rate constant, k_d, for the dehydration reaction, i.e. the release of one H_2O (or OH^-).

For the thermodynamic stability constant of the hydrated/hydroxy entities we use the values for the outer-sphere association, K^{os} ($m^3\ mol^{-1}$) computed on the basis of point charges [29], while accounting for the multi-site nature of the di- and tri-hydroxy entities [30-32]. Computations were performed for an ionic strength of 100 mol m^{-3} (with a corresponding Debye layer thickness $\kappa^{-1} = 9\times10^{-10}$ m), a charge separation distance of 0.5 nm within the ion pair, and T = 293 K. Values are given in Table 1.

Table 1: k_w, k_a and K^{os} values for aqueous In(III) species, I = 100 mol m^{-3}

In(III) species	$k_w = k_d$ / s^{-1} [(a)]	K^{os} / m^3 mol^{-1}	$k_a = k_w K^{os}$ / m^3 mol^{-1} s^{-1}
$In(H_2O)_6^{3+}$	200	3.15×10^{-4}	0.063
$In(H_2O)_5(OH)^{2+}$	10^5	5.18×10^{-3}	518
$In(H_2O)_4(OH)_2^{+}$	10^7	0.11	1.1×10^6
$In(H_2O)_3(OH)_3^{0}$	10^9	2.07	2.07×10^9

[(a)] the k_w values are those reported for Fe(III); see text for details

(De)protonation kinetics

The dynamic complexation features of the aqueous In(III) species are concerned with the protonation/deprotonation rates of water in the inner hydration sphere, together with the association/dissociation rate of the ions with protonated/deprotonated water. In *bulk* aqueous solution, the association/dissociation reaction for H_2O can be written as:

$$H^+ + OH^- \underset{k_{d,H_2O}}{\overset{k_{a,H_2O}}{\rightleftharpoons}} H_2O \qquad (1)$$

The values of the rate constants at 298 K have been reported as k_{a,H_2O} = 1.4×10^8 m^3 mol^{-1} s^{-1} and k_{d,H_2O} = 2.5×10^{-5} s^{-1} [33-35]. The magnitude of k_{a,H_2O} implies that the association reaction of H^+ and OH^- in bulk solution is diffusion limited. In such case, the rate constant can be calculated via [34]:

$$k_a = \frac{4\pi N_{Av} z^+ z^- e^2 (D_{H^+} + D_{OH^-})}{\varepsilon\varepsilon_0 kT[\exp(z^+ z^- e^2 / \varepsilon\varepsilon_0 akT) - 1]} \qquad [\text{m}^3\ \text{mol}^{-1}\ \text{s}^{-1}] \qquad (2)$$

where N_{Av} is the Avogadro number (6.022×10^{23} mol^{-1}), z is the charge on the respective ions, e is the elementary charge (1.6×10^{-19} C), $\varepsilon\varepsilon_0$ is the dielectric permittivity of the aqueous solution (= 7×10^{-10} F m^{-1} at 293 K), k is the Boltzmann constant (1.38×10^{-23} J K^{-1}), T is the temperature (K), a is the distance of closest approach (m), D_{H^+} = 9.3×10^{-10} m^2 s^{-1} and D_{OH^-} = 5.3×10^{-10} m^2 s^{-1} [36]. The k_a computed using Eq. 2 is approximately equal to the measured k_{a,H_2O} for a = 0.75 nm [34]. In present context, the various In(III) species comprise hydrated In^{3+} ions which differ in the extent to which H_2O is deprotonated in the inner hydration sphere. On a simple electrostatic basis, one might expect the release rate of water to be greater than that of OH^-. In practice the detailed picture may be more involved. Notably, the dissociation equilibrium of H_2O is strongly perturbed in the inner-hydration sphere of charged ions, and water speciation in the inner hydration sphere is highly dynamic with an OH^- being turned into an H_2O on a timescale much shorter than that for reorganization of the complex structure of the In(III) species. The rate of recombination of an OH^- in the inner-hydration sphere with a proton is essentially diffusion controlled and largely unaffected by the charge of the hydroxy complex [37,38]; the rate constant for this process for a trivalent ion is estimated to be *ca.* 5×10^6 m^3 mol^{-1} s^{-1} [38]. This value, together with the stepwise hydrolysis constants, K^*, of *ca.* 10^{-1} m^3 mol^{-1} for each of the In(III) species [39], enables the rate constant for loss of a proton from a given In(III) species

to be estimated as *ca.* 5×10^5 s^{-1} [6]. This value confirms that there will be rapid interchange between H_2O and OH^- in the inner-hydration sphere, whilst the equilibrium concentrations of the various In(III) species derive from the hydrolysis constants.

During an electrodic reduction process at a mercury electrode, the "free" In(III) ions are reduced to elemental In^0 and accumulate in the electrode volume. In the present case, electron transfer can occur with *all* the In(III) species, i.e. the overall electrodic reduction does not rely on interconversion with a singular electroactive species, and the "free" In(III) comprises *all* species that have lost one H_2O or OH^-. Whilst release of H_2O and/or OH^- is not a prerequisite for electron transfer, we proceed with the assumption that the electroactive form of *each* of the In(III) species is that which has lost (at least) one H_2O (protonated or deprotonated) from its inner hydration sphere. Support for this strategy is provided by the qualitative correlation observed between k_w and electron transfer reversibility (see Introduction and Table 1) which evidences the connection between lability and reversibility, in contrast to the option of a direct complex reduction of the pertaining complex species. In this context we highlight that an *n* electron process takes place via *n* distinct, albeit practically indistinguishable, electron transfer steps [40]. Each electron transfer step reduces the charge on the In ion, thereby facilitating the release of H_2O and OH^-, all of which are lost over the course of the reduction to metallic In^0. As documented above (Table 1), k_w increases as the metal ion becomes increasingly hydrolysed, and loss of the first water molecule from the inner-hydration sphere is generally the slowest step in the context of metal complexation kinetics [41].

The concept of *lability* describes the extent to which the various In(III) species can maintain equilibrium with each other in the context of the ongoing interfacial reduction process [17]. A given species is denoted as labile if it undergoes frequent interconversions with the electroactive form during its transport through the diffusion layer. In the present case, the consideration of lability refers to *both* (1) interconversions between the various fully hydrated species, i.e. protonation/deprotonation rate of inner-sphere water molecules, and (2) interconversion between the fully hydrated and partially dehydrated forms of a given species. Considering case (1), as discussed above, the rate constant for loss of a proton from each of the In(III) species is *ca.* 5×10^5 s^{-1}. The lifetime of the various species, $1/(5\times10^5\ s^{-1}) = 2\times10^{-6}$ s, is much shorter than the diffusion timescale of *ca.* 3 s given by δ^2/D_{In}, where δ is the thickness of the diffusion layer in solution ($\approx 5\times10^{-5}$ m for the hanging mercury drop electrode used herein with constant stirring of the solution during deposition [42]) and D_{In} is the diffusion coefficient ($= 8\times10^{-10}$ m^2 s^{-1} [2] for all In(III) species considered, i.e. since the diffusion layer thickness is much greater than the Debye screening length, κ^{-1}, we can neglect any effect of electrostatics on the diffusion of the various In(III) species towards the electrode surface [43]). Thus the various protonated/deprotonated species will maintain full equilibrium with each other in the steady-state diffusion layer throughout the electrodic reduction step.

(De)hydration kinetics

Considering interconversions between the fully hydrated and partially dehydrated forms of a given species – case (2) above – the pertaining k_w values are involved (Table 1), and the lability features of the various In(III) species are conveniently analysed by invoking the approximative reaction layer concept developed by Koutecký-Koryta (KK) [44-46]. The KK approximation has proven useful in describing the lability features of a wide range of metal complex systems [47-50]. The KK approach describes the transition from complexation equilibrium control (with coupled diffusion of all species) to kinetic control (with dissociation rate limitation) at the reaction layer boundary in the vicinity of a metal-consuming interface such as an electrode or an organism. The reaction layer concept derives from the relative mobilities and lifetimes of the various metal species in the medium. Conventionally, the reaction layer thickness, μ_i, for each species, i, derives from the mobility of the free ion in the medium (i.e. that which has lost one H_2O or OH^-) and its mean free lifetime, $1/k_{a,i}c_L$ (in present context, governed by the rate of re-association with a water molecule or an OH^-, see above) [51]:

$$\mu_i = \left(\frac{D_{In}}{k_{a,i} c_L} \right)^{1/2} \quad [m] \quad (3)$$

where c_L, is the concentration of the ligand, L, where L may be H_2O or OH^-, and refers to that of their free forms, i.e. not associated with In(III). For the case of $In(H_2O)_6^{3+}$, $c_L = c_{H_2O} = 5.55\times10^4$ mol m^{-3}, whilst for the various hydroxy species, c_L is c_{OH^-} according to the pH of the medium. For the case of $In(H_2O)_6^{3+}$, the lifetime of the free form $In(H_2O)_5^{3+}$ ($1/k_{a,i}c_L$) is 2.86×10^{-4} s, and the corresponding μ_i is 4.8×10^{-7} m (Eq. 3). When several In(III) species are simultaneously present, a combined μ can be formulated according to:

$$\mu = \left(\frac{D_{In}}{\left[\sum_i (1/k_{a,i} c_L) \right]^{-1}} \right)^{1/2} \quad [m] \quad (4)$$

More rigorously, the formulation of the reaction layer thickness should also take into account the mobility of the fully hydrated form and its mean free lifetime, $1/k_{d,i}$, (governed by the rate of release of water). The expression for such a generalised reaction layer thickness, λ_i, defined by both the associative and dissociative terms for a given species i, is given by [52, 53]:

$$\lambda_i = \left(\frac{k_{a,i} c_L}{D_{In}} + \frac{k_{d,i}}{D_{In}} \right)^{-1/2} \quad [m] \quad (5)$$

For the case of $In(H_2O)_6^{3+}$, its mean free lifetime, $1/k_{d,i}$, is 5×10^{-3} s, whilst that of the hydroxy species decreases with increasing degree of hydrolysis, i.e. increasing k_w values (Table 1). Eq. 5 can also be written in combined form to include the cumulative contributions to the free lifetime from the various species i:

$$\lambda = \left(\frac{\left[\sum_i (1/k_{a,i} c_L) \right]^{-1}}{D_{In}} + \frac{\left[\sum_i (1/k_{d,i}) \right]^{-1}}{D_{In}} \right)^{-1/2} \quad [m] \quad (6)$$

The conventional and generalised reaction layer thicknesses are given in Table 2 as a function of pH for each individual In(III) species. Note also that for $In(H_2O)_6^{3+}$, the $k_{a,i}$ term governs the thickness of its individual

reaction layer λ_i (Eq. 5), i.e. the lifetime of the free form, given by $1/k_{a,i}c_L$ (2.86×10^{-4} s), is less than that of the fully hydrated form, given by $1/k_{d,i}$ (5×10^{-3} s). The opposite holds for the various hydroxy species, i.e. the respective $k_{d,i}$ terms in Eq. 5 determine the reaction layer thickness. At each pH, the magnitude of the *combined* μ (Eq. 4) and the *combined* λ (Eq. 6) is approximately equal to the respective individual values for $In(H_2O)_6^{3+}$, which is a consequence of the low k_w for this species (Table 1). Due to the large differences in magnitude of the individual reaction layer thicknesses across the various In(III) species (Table 2), we proceed by considering the kinetic behaviour of each species to be governed by its *individual* reaction layer thickness. This approach is analogous to the situation of separate diffusion layers being operable for free and complexed metal species when their diffusion coefficients are very different, even if they are labile [54], and is supported by the experimental data reported herein (see Results and Discussion).

Table 2. Conventional, μ_i, and generalised, λ_i, reaction layer thicknesses for individual aqueous In(III) species, I = 100 mol m^{-3}

In(III) species	μ for individual species / m				λ for individual species / m			
	pH 1.8	pH 2.5	pH 3.0	pH 3.5	pH 1.8	pH 2.5	pH 3.0	pH 3.5
$In(H_2O)_6^{3+}$	4.8×10^{-7}	4.8×10^{-7}	4.8×10^{-7}	4.8×10^{-7}	4.65×10^{-7}	4.65×10^{-7}	4.65×10^{-7}	4.65×10^{-7}
$In(H_2O)_5(OH)^{2+}$	0.050	0.022	0.012	7.0×10^{-3}	8.9×10^{-8}	8.9×10^{-8}	8.9×10^{-8}	8.9×10^{-8}
$In(H_2O)_4(OH)_2^{+}$	1.07×10^{-3}	4.8×10^{-4}	2.7×10^{-4}	1.5×10^{-4}	8.9×10^{-9}	8.9×10^{-9}	8.9×10^{-9}	8.9×10^{-9}
$In(H_2O)_3(OH)_3^{0}$	2.5×10^{-5}	1.1×10^{-5}	6.2×10^{-6}	3.5×10^{-6}	8.9×10^{-10}	8.9×10^{-10}	8.9×10^{-10}	8.9×10^{-10}

The species distribution of In(III) in the bulk aqueous medium is computed using the literature cumulative hydrolysis constants, β^* (dm^3 mol^{-1}; average of 4 independent publications at ionic strength *ca.* 100 mM) [39, 55-57]: i.e. log β_1^* = -3.87, log β_2^* = -8.16, and log β_3^* = -12.6 (the formulation of these constants is given in the Supporting Information). The resulting speciation of In(III) as function of pH is shown in Fig. 1.

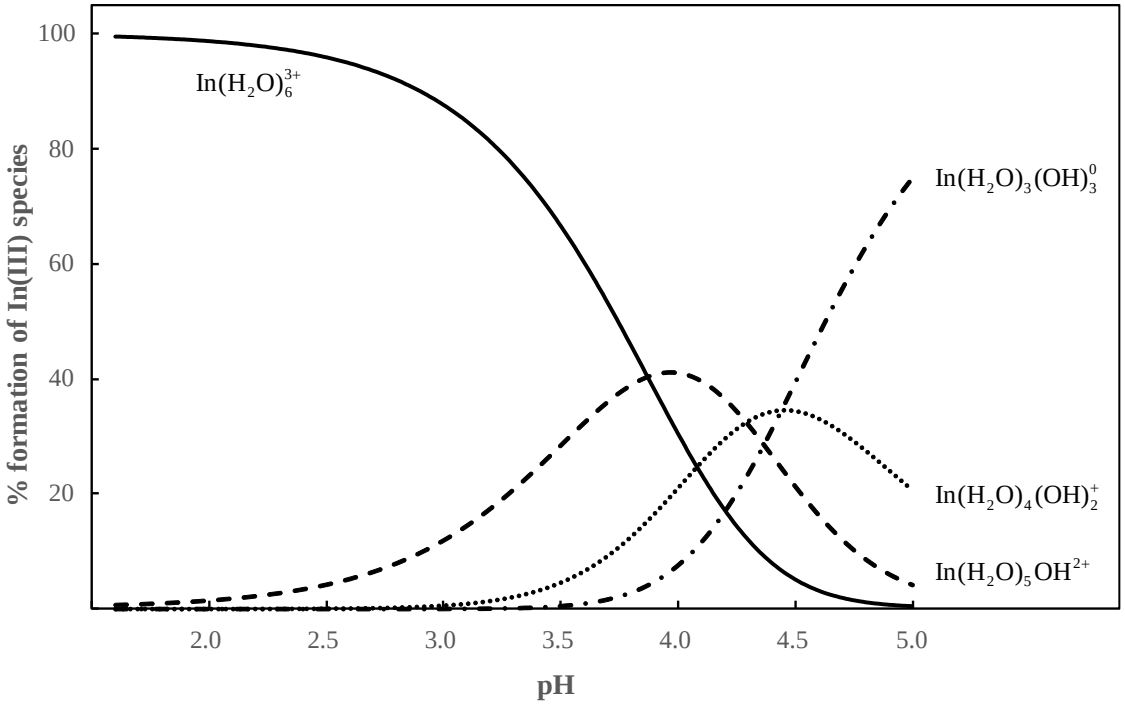

Fig. 1 Percent formation of aqueous In(III) species as a function of pH. Values were computed using hydrolysis constants from the literature: log β_1^* = -3.87, log β_2^* = -8.16, and log β_3^* = -12.6 (average values from 4 publications measured at ionic strength *ca*. 100 mM; see list of symbols for elaborated definitions of the β^* values) [39, 55-57]. As indicated on the figure, the various curves correspond to $In(H_2O)_6^{3+}$ (solid line), $In(H_2O)_5(OH)^{2+}$ (dashed line), $In(H_2O)_4(OH)_2^+$ (dotted line), and $In(H_2O)_3(OH)_3^0$ (dot-dashed line)

The kinetic flux for each In(III) species, $J_{\mathrm{kin},i}$, is given by :

$$J_{\mathrm{kin},i} = k_{\mathrm{w},i} c_i \lambda_i \qquad [\mathrm{mol\ m^{-2}\ s^{-1}}] \qquad (7)$$

where λ_i is the *individual* value in Table 2, and c_i is obtained from the hydrolysis constants (Fig. 1). The ensuing $J_{\mathrm{kin},i}$ values for each species as a function of pH are given in Table 3.

Table 3: Kinetic flux, $J_{\mathrm{kin},i}$, (Eq. 7) for individual In(III) species as a function of pH

In(III) species	$J_{\mathrm{kin},i}$ for each species, mol m^{-2} s^{-1}			
	pH 1.8	**pH 2.5**	**pH 3.0**	**pH 3.5**
$In(H_2O)_6^{3+}$	9.2×10^{-5}	8.9×10^{-5}	8.2×10^{-5}	6.1×10^{-5}
$In(H_2O)_5(OH)^{2+}$	7.4×10^{-5}	3.6×10^{-4}	1.04×10^{-3}	2.5×10^{-3}
$In(H_2O)_4(OH)_2^+$	0	8.9×10^{-5}	5.3×10^{-4}	4.1×10^{-3}
$In(H_2O)_3(OH)_3^0$	0	0	0	1.3×10^{-2}

Lability

As detailed above (see (De)protonation kinetics section), interconversions between the various protonated/deprotonated species are labile on the timescale of diffusion in the steady-state diffusion layer. Here

we assess the situation with respect to interconversions between the fully hydrated and partially dehydrated forms of each individual In(III) species. In this case, the lability parameter for each species, $\mathcal{L}_i$, is conveniently expressed as the ratio of the individual kinetic flux and the diffusive flux, $J_{\mathrm{kin},i}$ and J_{dif} respectively [17]:

$$\mathcal{L}_i = J_{\mathrm{kin},i}/J_{\mathrm{dif}} \quad (8)$$

where $J_{\mathrm{kin},i}$ (Eq. 7) corresponds to the rate of dissociation of the complexed form (i.e. that which is fully hydrated) into the free form (i.e. that which has lost one H_2O or OH^-), and J_{dif} is the diffusion-limited flux of all the In(III) species from bulk solution to the electrode, given by:

$$J_{\mathrm{dif}} = D_{\mathrm{In}} c^*_{\mathrm{In,t}} / \delta \qquad [\mathrm{mol\ m^{-2}\ s^{-1}}] \quad (9)$$

where $c^*_{\mathrm{In,t}}$ (mol m^{-3}) is the total concentration of In(III) in the bulk aqueous medium.

A given species is labile if $\mathcal{L}_i >> 1$ [17]. The lability parameter (Eq. 8) for each In(III) species with respect to interconversions between its fully and partially dehydrated forms in the pH range 1.8 to 3.5 follow as: $In(H_2O)_6^{3+}$: $\mathcal{L}_i$ = 6 to 4; $In(H_2O)_5(OH)^{2+}$: $\mathcal{L}_i$ = 5 to 156; $In(H_2O)_4(OH)_2^{+}$: $\mathcal{L}_i$ = 6 to 256; and $In(H_2O)_3(OH)_3^{0}$: $\mathcal{L}_i$ = 812. Thus full equilibrium will be maintained between the various (partially) hydrated forms of each individual In(III) species in the steady-state diffusion layer throughout the electrodic reduction step.

Electrochemical reactivity

All In(III) species will contribute to the overall electrodic reduction to an extent determined by the relative magnitudes of their diffusive flux towards the electrode, their rate of release of H_2O and/or OH^-, and their rate of electron transfer. Thus, for present purposes of describing the electrochemical reactivity, it is necessary to compare the rate of supply of each individual species, *i*, in its individual reaction layer, λ_i (Table 2) versus its rate of electron transfer, i.e. $\min(D_{\mathrm{In}} c_i / \lambda_i, k_{\mathrm{d},i} c_i \lambda_i)$ versus $k_i^0 c_i$, where k_i^0 is the rate constant for electron transfer (m s^{-1}), c_i (mol m^{-3}) is obtained from the hydrolysis constants (see above and Fig. 1), and as before, D_{In} is the same for all species (8×10^{-10} m^2 s^{-1}). The rate of supply of each species to the electrode surface will be rate limiting when $k_i^0 >> \min(D_i / \lambda_i, k_{\mathrm{d},i}\lambda_i)$. Meeting this criterion requires k^0 ($In(H_2O)_6^{3+}$) >> 9×10^{-5} m s^{-1}, k^0 ($In(H_2O)_5(OH)^{2+}$) >> 9×10^{-3} m s^{-1}, k^0 ($In(H_2O)_4(OH)_2^{+}$) >> 0.09 m s^{-1}, and k^0 ($In(H_2O)_3(OH)_3^{0}$) >> 0.9 m s^{-1}.

Values of k_i^0 in the range 10^{-11} to 10^{-14} m s^{-1} have been derived for $In(H_2O)_6^{3+}$ from measurements with a dropping mercury electrode in acidic media [2, 58]. Thus the rate of electron transfer is the rate limiting step in the reduction of $In(H_2O)_6^{3+}$, and its contribution to the overall electrodic reduction will be limited by its slow rate of electron transfer in agreement with experimental data [2-4]. As the pH is increased to values at which hydroxy species are present in non-negligible concentrations, a reversible reduction process is detected at potentials much more positive than those at which the irreversible reduction of $In(H_2O)_6^{3+}$ occurs. The reversible wave reported at $E_{1/2}$ of -0.55 V (*vs*. SCE) [2-4] indicates that the contribution of the various In(III)

hydroxy species to the overall electrodic reduction is governed by their rate of diffusion towards the electrode surface (also see Results and Discussion). The differences between the various In(III) species in terms of the relative rates of the elementary processes governing electrochemical reactivity, determine their relative contributions to the overall electrodic reduction. As an illustrative example, at pH 1.8, for a total In(III) concentration of 10^{-3} mol m^{-3}, the concentration of $In(H_2O)_6^{3+}$ is 9.92×10^{-4} mol m^{-3} and of $InOH^{2+}$ is 8×10^{-6} mol m^{-3} (Fig. 1), thus the contribution of the irreversible reduction of $In(H_2O)_6^{3+}$ to the overall electrodic reduction will be *ca.* 7 orders of magnitude lower than that of the reversible reduction of $In(H_2O)_5(OH)^{2+}$, even using the highest reported value of k_i^0 for $In(H_2O)_6^{3+}$ of 10^{-11} m s^{-1}. Specifically, $J_{In(H_2O)_6^{3+}}$ (electron transfer limited rate in the reaction layer) = 10^{-11} m s^{-1} × 9.92×10^{-4} mol m^{-3} = 9.92×10^{-15} mol m^{-2} s^{-1}, *cf.* $J_{In(H_2O)_5OH^{2+}}$ (diffusive flux in the reaction layer) = 8×10^{-10} m^2 s^{-1} × 8×10^{-6} mol m^{-3} / 8.9×10^{-8} m = 7.2×10^{-8} mol m^{-2} s^{-1}.

Experimental

Reagents

All solutions were prepared in distilled, deionised water from a Milli-Q system (resistivity > 18 MΩ cm). Test solutions containing 5.6×10^{-4} mol m^{-3} In(III) were prepared by dilution of a standard (TraceCERT, Sigma-Aldrich). Ionic strength was maintained at 100 mM with $NaClO_4$, prepared from the solid (puriss p.a.). Perchlorate ions do not form inner-sphere complexes with In(III) [59], and do not specifically adsorb on Hg in the potential range used herein [60]. The pH of the test solutions was adjusted to the target value by addition of $HClO_4$ and NaOH, and remained constant over the duration of the experiments.

Electrochemical measurements

The electrochemical measurements were performed with an Ecochemie μAutolab potentiostat (input impedance > 100 GΩ) coupled with a Metrohm VA stand. The working electrode was a multimode hanging mercury drop electrode (HMDE) with radius *ca.* 2×10^{-4} m, the auxiliary electrode was glassy carbon, and the reference electrode was Ag|AgCl|KCl(sat) encased in a 100 mM $NaClO_4$ jacket. Solutions were initially purged with oxygen-free N_2 and a nitrogen blanket was maintained during measurements. Stripping chronopotentiometric measurements were performed over a range of deposition potentials, E_d, i.e. the solution is stirred and the electrode potential is held at the chosen E_d for a fixed deposition time, t_d, during which In^0 accumulates in the Hg electrode; at the end of the t_d, a stripping (oxidising) current, I_s, is applied in quiescent solution until the potential reaches a value well past the transition plateau. The area under the recorded dt/dE *vs.* E curve corresponds to the stripping time, τ. A stripping current of 2 nA was used which corresponds to complete depletion conditions for the HMDE used herein [61]. Stripping chronopotentiometry at scanned deposition potential (SSCP) comprises plots of τ as a function of E_d. Such SSCP waves, analogous to conventional voltammograms, scan the relevant parts of the stability distribution and the rate constant distributions. An overview of the fundamental principles of SSCP is given in the Supporting Information and

the reader is referred to our previous work for further details of the SSCP methodology and the advantages of the complete depletion regime for metal speciation analysis [62-65].

Results and Discussion

Reversibility of the electrodic reduction

Voltammetric waves recorded for In(III) show an irreversible wave for $In(H_2O)_6^{3+}$ ($E_{1/2}$ = -0.95V *vs*. SCE) when the pH is sufficiently low to suppress hydrolysis; as the pH is increased to values at which hydroxy species are present in solution a reversible diffusion-controlled wave appears ($E_{1/2^{rev}}$ -0.55 V *vs*. SCE) [2-4]. This behaviour was also observed in the present work (Fig. S1). The transition from reversible to irreversible electrochemical behaviour depends on the timing characteristics of the technique, which for SSCP corresponds to k^0 values in the range from *ca*. 10^{-4} to 10^{-6} m s^{-1} [47]. That is, once k^0 is of $O(10^{-6})$ m s^{-1} or less, the slope of a $\log[\tau^*-\tau)/\tau]$ vs. E_d plot (where τ^* is the limiting value of τ obtained when the concentration of the electroactive species at the electrode surface essentially equals zero) is independent of t_d, and lower than that for the reversible case [47]. SSCP curves recorded for In(III) as a function of pH feature two distinct waves with half-wave deposition potentials $E_{d,1/2}$ of *ca*. -0.56 V and *ca.* -0.95 V; Fig. 2. The wave with $E_{d,1/2} \approx$ -0.56 V is ascribed to reversible reduction of In(III) hydroxy species (see further discussion below), whilst the drawn-out wave with $E_{d,1/2} \approx$ -0.95 V corresponds to irreversible reduction of $In(H_2O)_6^{3+}$.

As the pH is increased from 1.8 to 3.1, the height of the first plateau increases, and that of the second decreases. At higher pH, the slight decrease in the height of the first wave may reflect the formation of multi-nuclear hydroxy species with a somewhat lower diffusion coefficient than the mononuclear ones and/or low solubility: precipitation of In(III) hydroxy species begins at pH *ca.* 3.4 [66]. The decrease in the height of the plateau at E_d -1.25 V with increasing pH reflects the decreasing concentration as well as the increasing irreversibility of the $In(H_2O)_6^{3+}$ species. At pH 1.8, the magnitude of τ at an E_d of -1.25 V corresponds to the value predicted on the basis of the diffusive flux of the total In(III), in line with the conventional overcoming of irreversibility at extreme overpotentials [40].

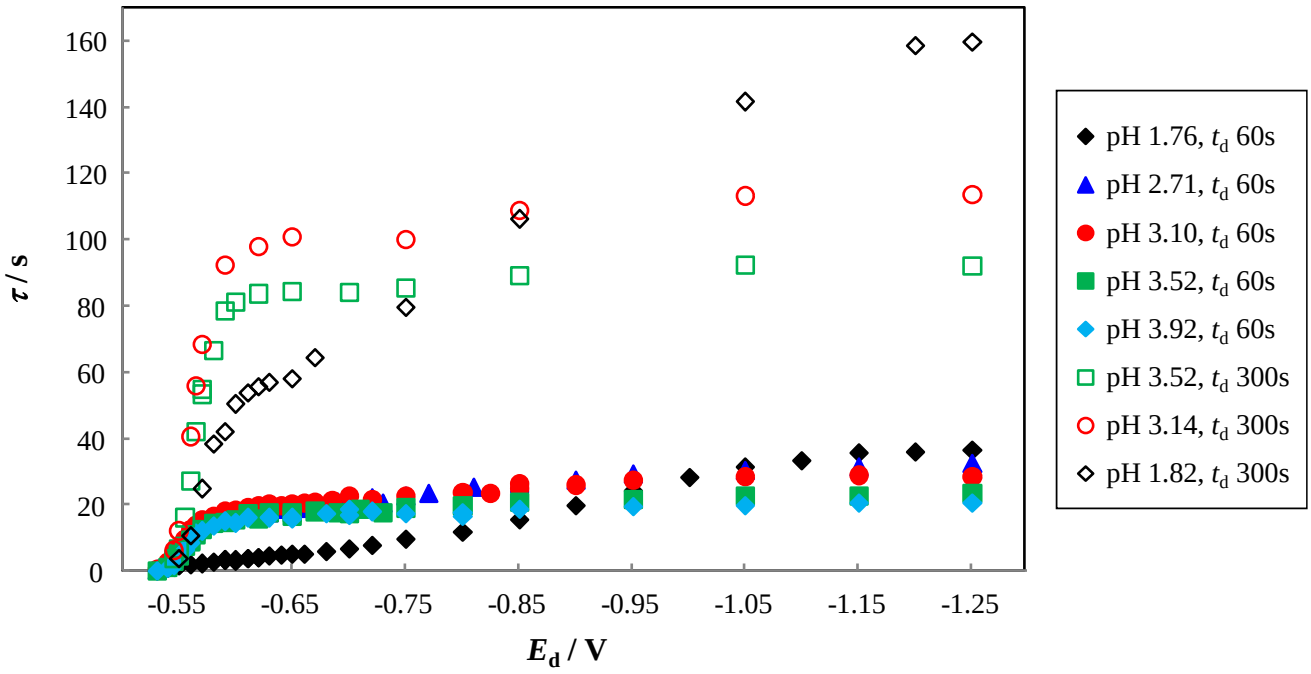

Fig. 2 SSCP waves for In(III) as a function of pH for a deposition time, t_d, of 60 s (solid symbols) and 300 s (open symbols). Total concentration of In(III) = 5.6×10^{-4} mol m^{-3}, I = 100 mol m^{-3} $NaClO_4$

Estimation of k^0 for In(III) hydroxy species

The full SSCP curve of τ versus E_d is given by [22]:

$$\tau = \frac{I_d^* \tau_d}{I_s}\left[1-\exp(-t_d/\tau_d)\right] \quad [s] \qquad (10)$$

where I_d^* (A) is the limiting value of the deposition current obtained when the concentration of the electroactive species at the electrode surface essentially equals zero, and τ_d (s) is the potential-dependent time constant of the deposition process. With appropriate elaborations of the I_d^* and τ_d terms, Eq. 10 has been demonstrated to describe the SSCP waves measured for a wide range of metal complex systems, including those involving kinetic currents [47, 49], heterogeneity in the chemical speciation [48, 62], and electrochemical irreversibility [23, 67]. In the case of nonreversible electron transfer processes, the expressions for the general quasi-reversible case are [23, 67]:

$$I_d^* = \frac{nFAk^0}{1+nFAk^0 m_{In}\theta_\alpha} c_{In,t}^* \theta_\alpha \quad [A] \qquad (11)$$

and

$$\tau_d = \frac{nFVm_{In}}{\theta} + \frac{nFV}{nFAk^0\theta_\beta} \quad [s] \qquad (12)$$

where A and V are the surface area and volume of the electrode, respectively, $m_{In} = \delta / nFAD_{In}$, $\theta = \exp[nF(E_d - E^{0'})/RT]$ where $E^{0'}$ is the formal potential, $\theta_\alpha = \exp(-\alpha y)$ and $\theta_\beta = \exp(\beta y)$ where α is the charge transfer coefficient, $\beta = 1 - \alpha$, and $y = nF(E_d - E^{0'})/RT$. Eq. 11 has sound limits: for very fast

mass transport, $m_{In} \rightarrow$ zero and $I_d^* \rightarrow nFAk^0 c_{In,t}^* \exp(-\alpha y)$, i.e. the totally irreversible current, whilst for electrochemically reversible systems with $nFAk^0 c_{In,t}^* \exp(-\alpha y) >> 1$, $I_d^* \rightarrow c_{In,t}^* / m_{In}$, i.e. the diffusive limiting current. Eqs. 10, 11, and 12 evidence that the shape of the SSCP wave for a quasi-reversible electrodic reduction is sensitive to the magnitude of k^0, and a steepening of the wave with increasing t_d is a characteristic feature of such systems [23, 67].

For the case of In(III) at pH values greater than *ca.* 2.5, the shape of the SSCP wave with $E_{d,1/2}$ *ca.* -0.56 V is practically independent of t_d. Comparison with computed curves (Eqs. 10, 11, and 12; Fig. 3) establishes that at pH values above *ca.* 2.5 the electrodic reduction of the In(III) hydroxy species is practically reversible ($k^0 \rightarrow \infty$), whilst at pH 1.8 the effective rate constant for electron transfer, k_{eff}^0, is of the order of 10^{-5} m s^{-1}.

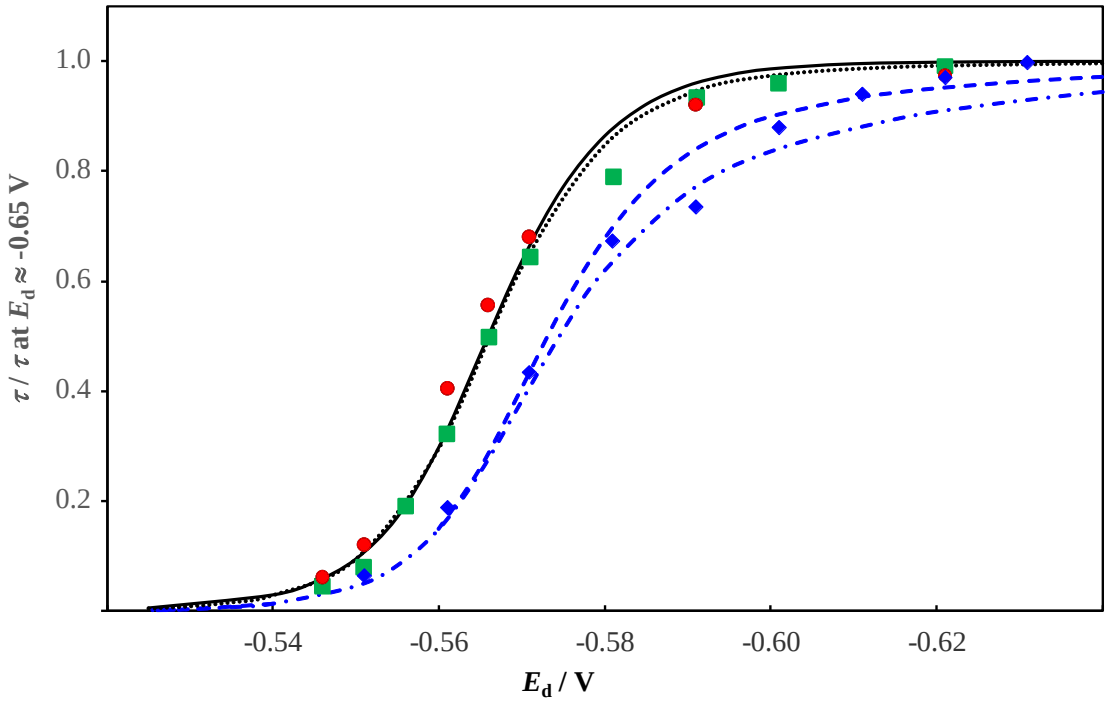

Fig. 3 SSCP curves normalised with respect to τ measured at an E_d of *ca.* -0.65 V. Deposition time, t_d = 300s. Symbols correspond to experimental data at pH 1.82 (blue diamonds), 3.14 (red dots), and 3.52 (green squares). The lines correspond to computed curves for the reversible case with $E^{0'}$ = -0.534 V (solid black line), the quasi-reversible case with $k^0 = 2\times10^{-4}$ m s^{-1} and $E^{0'}$ = -0.534 V (black dotted line), $k^0 = 4\times10^{-5}$ m s^{-1} and $E^{0'}$ = -0.540 V (blue dashed line), and $k^0 = 2\times10^{-5}$ m s^{-1} and $E^{0'}$ = -0.540 V (blue dot-dashed line). Computations were performed for n = 3, α = 0.22 [2, 58]

Estimation of k^0 for $In(H_2O)_6^{3+}$

The observed irreversibility of the $In(H_2O)_6^{3+}$ wave ($E_{d,1/2} \approx$ -0.95 V) is in agreement with the predicted behaviour of this species (see Introduction and Theory sections). In this context it is relevant to note that the reported k^0 values for $In(H_2O)_6^{3+}$ of 10^{-11} to 10^{-14} m s^{-1} [2, 58] are so-called 'true' values. Since reduction of

In(III) species takes place at potentials that are negative of the pzc of the mercury electrode (*ca.* -0.5 V [60]), the magnitude of the Frumkin correction must also be considered in assessment of the reversibility of the electrodic reduction process. The effective rate constant for electron transfer, k^0_{eff}, can be computed from the true value, k^0, via [40]:

$$k^0_{\text{eff}} = k^0 \exp[(\alpha n - z)F\psi_{\text{OHP}} / RT] \quad (13)$$

where α is the charge transfer coefficient, n is the number of electrons transferred, z is the charge on the ionic species, F is the Faraday constant (96485 C mol^{-1}), ψ_{OHP} is the potential at the outer Helmholtz plane (V), R is the gas constant (8.314 J K^{-1} mol^{-1}), and T is the temperature (K). In this context we highlight that there is no specific adsorption of electrolyte perchlorate anions, OH^- or H^+ ions on the Hg electrode over the potential range considered [60], and perchlorate ions do not form inner-sphere complexes with In(III) [59]. For the case of In(III) in acidic perchlorate media, αn is 0.66 [2,58], and for a mercury electrode at an applied potential of -0.60 V in acidic perchlorate media, ψ_{OHP} is *ca.* -0.03 V [68]. Using Eq. 13, these values yield a k^0_{eff} for $In(H_2O)^{3+}_6$ at E_d = -0.60V that is *ca.* 16 times greater than the true value, and still many orders of magnitude below that of a reversible electrodic reduction process. This finding confirms that the wave with $E_{d,1/2} \approx$ -0.56 V can be ascribed to reduction of hydroxy In(III) species.

The SSCP waves recorded at pH 1.8 (Fig. 2) show that the height of the first plateau – corresponding to quasi-reversible reduction of In(III) hydroxy species (Fig. 3) – increases to a greater extent than expected on the basis of the increased t_d (for a reversible electrochemical reaction the SCP τ in the plateau region is directly proportional to t_d [22]), and the slope of the first wave becomes somewhat steeper. In the case of (quasi)-reversible systems, a longer t_d serves to shift the location of the SSCP wave on the potential axis to more negative values, thus the observed features are analogous to the conventional overcoming of irreversibility by going to more extreme potentials. The reader is referred to our previous work for more detailed explanation of this feature of SSCP [23, 69]. This aspect is highlighted in Fig. 4, which shows the SSCP waves recorded at pH 1.8 for several t_d, normalised relative to τ at -1.2 V. Once k^0 becomes less than O(10^{-6}) m s^{-1}, the electrodic process is irreversible on the SSCP timescale. The shape of an irreversible SSCP wave and its position on the E_d axis are invariant with t_d [23]. The data shown in Fig. 4 show that the slope and position on the potential axis of the electrodic reduction process occurring at the most negative deposition potentials is approximately invariant with t_d, thereby confirming the irreversibility of the pertaining process, i.e. reduction of $In(H_2O)^{3+}_6$. The SSCP wave for an irreversible process shifts to increasingly more negative E_d as k^0 decreases, by a factor of *ca.* 50 mV per 10-fold decrease in k^0 [23, 67]. These features enable us to estimate the k^0_{eff} for $In(H_2O)^{3+}_6$: at pH 1.8, the wave for the In(III) hydroxy species at $E_{d,1/2}$ *ca.* -0.56 V corresponds to k^0_{eff} *ca.* 2×10^{-5} m s^{-1} (Fig. 3), and the $E_{d,1/2}$ for the irreversible wave for $In(H_2O)^{3+}_6$ is located *ca.* 0.4 V more negative, and thus the corresponding k^0_{eff} will be *ca.* 8 orders of magnitude lower, i.e. *ca.* 10^{-13} m s^{-1}, in agreement with literature values [2, 58].

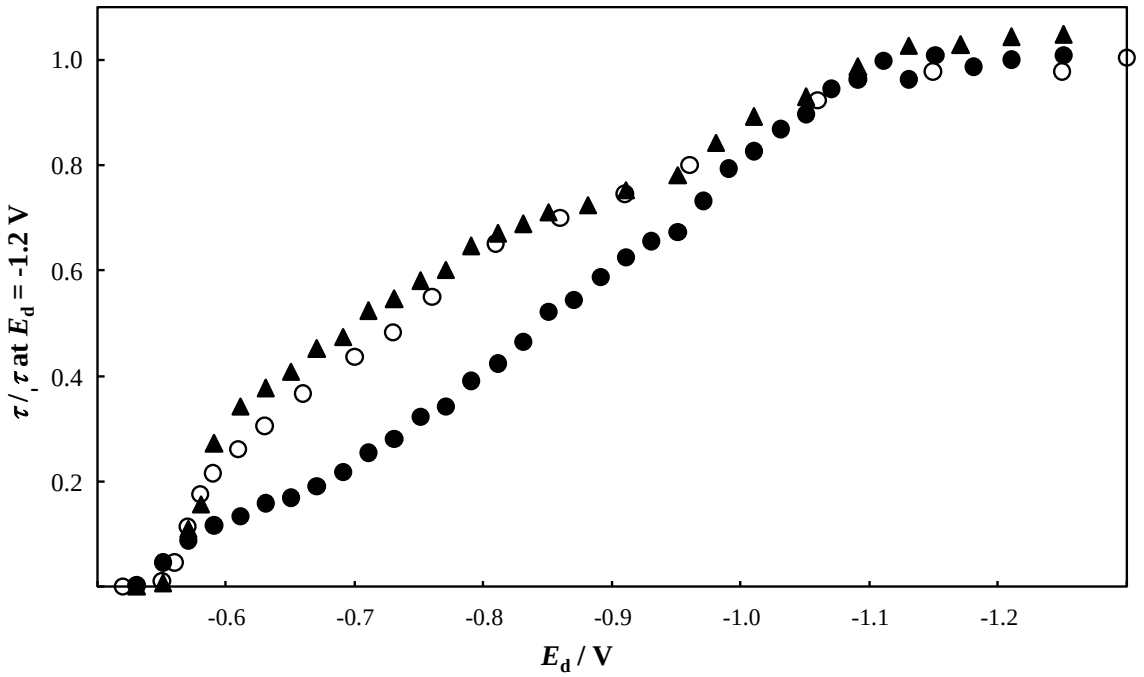

Fig. 4 SSCP waves for In(III) at pH 1.8 normalised relative to τ at E_d = -1.2 V for a deposition time, t_d, of 60 s (solid circles), 180 s (open circles), and 300 s (solid triangles). Total concentration of In(III) = 5.6×10^{-4} mol m^{-3}, I = 100 mol m^{-3} $NaClO_4$

Consequences for speciation analysis of In(III)

The preceding discussion evidences the irreversibility of the electrodic reduction of $In(H_2O)_6^{3+}$. Our results have consequences for interpretation of stripping chronopotentiometric data that purport to measure exclusively the $In(H_2O)_6^{3+}$ species at a potential of -0.58 V (corresponding to the foot of the SSCP wave recorded with a mercury film electrode) [10]. It is evident from the results presented herein that at such a potential only the In(III) hydroxy species will contribute significantly to the electrodic reduction. Furthermore, the decrease in τ measured at an E_d of -0.58 V with increasing pH has been erroneously interpreted as reflecting the decrease in the concentration of $In(H_2O)_6^{3+}$ [10]. Our findings show that such data rather reflect the shift in the reversible reduction wave for the In(III) *hydroxy* species towards more negative potentials as their degree of formation increases with increasing pH (i.e. increasing c_{OH^-} in the aqueous medium; Fig. 1), as described by the DeFord-Hume equation [70]. Specifically, an increase in pH from 2.8 to 3.5 would shift the reduction wave by -2.5 mV (computed using the literature hydrolysis constants given above); at a given potential corresponding to, say, 5% of the wave height at pH 2.8, the reduction current would be *ca.* 25 % lower at the same potential at pH 3.5. This value is in remarkable agreement with the reported *ca.* 23 % decrease in the "concentration of $In(H_2O)_6^{3+}$" derived from the decrease in magnitude of the SCP τ value over this pH range [10]; our results underscore that the published data [10] simply reflect the contribution from the In(III) hydroxy species. Evidently, our findings call for reinterpretation of the recent literature [9-11].

Conclusions and Outlook

The interpretation framework presented herein provides a straightforward means to characterise the electrochemical reactivity of aqueous ions together with their various hydrolysed counterparts. The theory is illustrated with experimental data for In(III). Specifically, invoking a Koutecky-Koryta type approximation for the reaction layer adjacent to the electrode/medium interface enables differences in reactivity of the aqueous In(III) species to be described according to their relative rates of electron transfer, dehydration, and/or (de)protonation. All In(III) species are found to be labile on the experimental timescale with respect to (de)protonation and (de)hydration, but large differences show up in to the rates of electron transfer. In the case of $In(H_2O)_6^{3+}$, the rate of electron transfer is found to be so slow that it replaces the traditional Eigen rate-limiting water release step in the overall passage from $In(H_2O)_6^{3+}$ to In^0. In contrast, the In(III) hydroxy species display reversible electrochemical behaviour. SSCP waves, which record the electrochemical reactivity as a function of reduction potential, are shown to be a useful tool for exploring the features of such systems. The results are of great consequence for electrochemical speciation analysis of In(III) and other hydrolysable ions, i.e. characterisation of all elementary processes which contribute to the electrochemical reactivity of all species is fundamental for robust data interpretation.

List of Symbols and Abbreviations

Latin

a	distance of closest approach of ions (m)
A	electrode surface area (m^2)
c_i	concentration of species i (mol m^{-3})
$c^*_{In,t}$	total concentration of In(III) in the bulk aqueous medium (mol m^{-3})
D	diffusion coefficient (m^2 s^{-1})
e	elementary charge (1.6×10^{-19} C)
E_d	deposition potential (V)
$E_{d,1/2}$	half-wave deposition potential (V)
$E_{1/2}$	half-wave potential (V)
$E^{0'}$	formal potential (V)
F	Faraday's constant (96485 C mol^{-1})
HMDE	hanging mercury drop electrode
I	ionic strength (mol m^{-3})
I^*_d	limiting value of the deposition current (A)
I_s	stripping current (A)
J_{dif}	diffusion controlled flux from the bulk medium to the electrode surface (mol m^{-2} s^{-1})
J_{kin}	kinetically controlled flux in the reaction layer (mol m^{-2} s^{-1})
k	Boltzmann constant (1.38×10^{-23} J K^{-1})
k_a	association rate constant (m^3 mol^{-1} s^{-1})

468	k_d	dissociation rate constant (s^{-1})
469	k^0	electron transfer rate constant (m s^{-1})
470	k^0_{eff}	effective electron transfer rate constant (m s^{-1})
471	KK	Koutecký-Koryta
472	K^{os}	stability constant for an outer-sphere reactant pair (m^3 mol^{-1})
473	k_w	inner-sphere dehydration rate constant of hydrated metal ions (s^{-1})
474	L	ligand
475	$\mathcal{L}$	lability parameter (dimensionless)
476	m_{In}	charge transport coefficient for In in aqueous solution
477	n	number of electrons transferred in the electrochemical reaction
478	N_{Av}	Avogadro number (6.022×10^{23} mol^{-1})
479	OHP	outer Helmholtz plane
480	R	gas constant (8.314 J K^{-1} mol^{-1})
481	SCE	saturated calomel electrode
482	SSCP	stripping chronopotentiometry at scanned deposition potential
483	t_d	deposition time (s)
484	T	temperature (K)
485	V	electrode volume (m^3)
486	y	$nF(E_d - E^{0'})/RT$
487	z	charge on an ion
488		
489	Greek	
490	α	charge transfer coefficient
491	β	$1 - \alpha$
492	β_1^*	stability constant for the reaction $In(H_2O)_6^{3+} \rightleftharpoons In(H_2O)_5(OH)^{2+} + H^+$
493	β_2^*	stability constant for the reaction $In(H_2O)_6^{3+} \rightleftharpoons In(H_2O)_4(OH)_2^{+} + 2H^+$
494	β_3^*	stability constant for the reaction $In(H_2O)_6^{3+} \rightleftharpoons In(H_2O)_3(OH)_3^{0} + 3H^+$
495	δ	thickness of the diffusion layer in solution at the electrode/medium interface (m)
496	$\varepsilon\varepsilon_0$	dielectric permittivity of the aqueous solution (7×10^{-10} F m^{-1} at 293 K)
497	θ	$\exp(y)$
498	θ_α	$\exp(-\alpha y)$
499	θ_β	$\exp(\beta y)$
500	κ^{-1}	Debye layer thickness (screening length) in the bulk electrolyte medium (m)
501	λ	thickness of the generalised reaction layer at the electrode/medium interface (m)
502	μ	thickness of the conventional association reaction layer at the electrode/medium interface (m)
503	τ	SCP transition (stripping) time (s)

504 τ_d characteristic time constant of the SCP deposition process (s)

505 ψ_{OHP} potential at the outer Helmholtz plane (V)

506

507 # References

1. Tuck DG (1983) Critical survey of stability constants of complexes of indium. Pure Appl Chem 55:1477-1528
2. Inouye S, Imai H (1960) Electrode kinetics of indium(III) at the dropping mercury electrode. Bull Chem Soc Jpn 33:149-152
3. Moorhead ED, MacNevin WM (1962) The polarographic behavior of indium in presence of chloride. Anal Chem 34:269-271
4. Engel A.J, Lawson J, Aikens DA (1965) Ligand-catalyzed polarographic reduction of indium(III) for determination of halides and certain organic sulfur and nitrogen compounds. Anal Chem 37:203-207
5. Losev VV, Molodov AI (1962) Einfluss der Säurekonzentration auf die Anodische Auflösung des Indiumamalgams. Electrochim. Acta 6:81-91
6. Lawson JG, Aikens DA (1967) Mechanism and thermodynamics of the polarographic deposition of aquo In(III). J Electroanal Chem 15:193-209
7. Nazmutdinov RR, Zinkicheva TT, Tsirlina GA, Kuz'minova ZV (2005) Why does the hydrolysis of In(iII) aquacomplexes make them electrochemically more active? Electrochim Acta 50:4888-4896
8. White SJO, Hemond HF (2012) The anthrobiogeochemical cycle of indium: a review of the natural and anthropogenic cycling of indium in the environment. Crit Rev Environ Sci Technol 42 :155-186
9. Tehrani MH, Companys E, Dago A, Puy J, Galceran J (2018) Free indium concentration determined with AGNES. Sci Total Environ 612 :269-275
10. Rotureau E, Pla-Vilanova P, Galceran J, Companys E, Pinheiro JP (2019) Towards improving the electroanalytical speciation analysis of indium. Anal Chim Acta 1052:57-64
11. Tehrani MH, Companys E, Dago A, Puy J, Galceran J (2019) New methodology to measure low free indium (III) concentrations based on the determination of the lability degree of indium complexes. Assessment of $In(OH)_3$ solubility product. J Electroanal Chem 847:113185.
12. Brun NR, Christen V, Furrer G, Fent K (2014) Indium and indium tin oxide induce endoplasmic reticulum stress and oxidative stress in zebrafish (*Danio rerio*). Environ Sci Technol.48:11679-11687
13. Brun NR, Fields PD, Horsfield S, Mirbahai L, Ebert D, Colbourne JK, Fent K (2019) Mixtures of aluminum and indium induce more than additive and toxicogenomic responses in *Daphnia magna*. Environ Sci Technol 53:1639-1649
14. Syun C-H, Chien P-H, Huang C-C, Jiang P-Y, Juang K-W, Lee D-Y (2017) The growth and uptake of Ga and In of rice (*Oryza sative* L.) seedlings as affected by Ga and In concentrations in hydroponic cultures. Ecotoxicol Environ Safety 135:32-39
15. Chang H-F, Wang S-L, Lee D-C, Hsiao SS-Y, Hashimoto Y, Yeh K-C (2020) Assessment of indium toxicity to the model plant Arabidopsis. J Haz Mat 387:121983
16. Yang G, Hadioui M, Wang Q, Wilkinson KJ (2019) Role of pH on indium bioaccumulation by *Chlamydomonas reinhardtii*. Environ Poll 250:40-46
17. van Leeuwen HP, Town RM, Buffle J, Cleven RFMJ, Davison W, Puy J, van Riemsdijk WH, Sigg L (2005) Dynamic speciation analysis and bioavailability of metals in aquatic systems. Environ Sci Technol 39:8545-8556
18. Morel FMM, Hering JG (1993) Principles and applications of aquatic chemistry. Wiley, New York
19. Zelić M, Mlakar M, Branica M (1994) Influence of perchlorates and halides on the electrochemical propertes of indium(III). Anal Chim Acta 289:299-306
20. Ashworth C, Firsch G (2017) Complexation equilibria of indium in aqueous chloride, sulfate and nitrate solutions: an electrochemical investigation. J Solution Chem 46:1928-1940
21. Jain DS, Gaur JN (1967) Reduction of indium at the dropping mercury electrode in lithium chloride medium. Electrochim Acta 12:413-416
22. van Leeuwen HP, Town RM (2002) Stripping chronopotentiometry at scanned deposition potential (SSCP). Part 1. Fundamental features. J Electroanal Chem 536:129-140
23. Town RM, van Leeuwen HP (2003) Stripping chronopotentiometry at scanned deposition potential (SSCP). Part 2. Determination of metal ion speciation parameters. J Electroanal Chem 541:51-65
24. van Leeuwen HP, Town RM (2003) Stripping chronopotentiometry at scanned deposition potential (SSCP). Part 3. Irreversible electrode reactions. J Electroanal Chem 556:93-102

25. Maeda M, Ohtaki H (1977) An X-ray diffraction study on the structure of the aqua indium(III) ion in the perchlorate solution. Bull Chem Soc Jpn 50:1893-1894
26. Lindqvist-Reis P, Munoz-Páez A, Díaz-Moreno S, Pattanaik S, Persson I, Sandström M (1998) The structure of the hydrated gallium(III), indium(III), and chromium(III) ions in aqueous solution. A large angle X-ray scattering and EXAFS study. Inorg Chem 37:6675-6683
27. Neely JW (1971) Oxygen-17 nuclear magnetic resonance studies of the first hydration sphere of diamagnetic metal ions in aqueous solution. PhD thesis, Lawrence Berkeley National Laboratory
28. Eigen M (1963) Fast elementary steps in chemical reaction mechanisms. Pure Appl Chem 6:97-115
29. Fuoss RM (1958) Ionic association. III. The equilbrium between ion pairs and free ions. J Am Chem Soc 80:5059-5061
30. van Leeuwen HP, Town RM, Buffle J (2007) Impact of ligand protonation in Eigen-type metal complexation kinetics in aqueous systems. J Phys Chem A 111:2115-2121
31. van Leeuwen HP (2008) Eigen kinetics in surface complexation of aqueous metal ions. Langmuir 24:11718-11721
32. van Leeuwen HP, Town RM (2009) Outer-sphere and inner-sphere ligand protonation in metal complexation kinetics: the lability of EDTA complexes. Environ Sci Technol 43:88-93
33. Eigen M, De Maeyer L (1955) Die Geschwindigkeit der Neutralisationsreaktion. Naturwissen 42:413-414
34. Eigen M, De Maeyer L (1958) Self-dissociation and protonic charge transport in water and ice. Proc R Soc (London) Ser A 247:505-533
35. Stillinger FH (1978) Proton transfer reactions and kinetics in water. In: Theoretical chemistry: advances and perspectives, vol. 3, 177-234
36. Light TS, Licht S, Bevilacqua AC, Morash KR (2005) The fundamental conductivity and resistivity of water. Electrochem Solid-State Lett 8: E16-E19
37. Eigen M, Kruse W (1963) Über den Einfluβ von Wassersoffbrücken-Struktur und elektrostatischer Wechselwirkung auf die Geschwindigkeit protolytischer Reaktionen. Z Naturforsch B 18:857-865
38. De Maeyer L, Kustin K (1963) Fast reactions in solution. Ann Rev Phys Chem 14:5-34
39. Alekseev VG, Myasnikova EN, Nikol'skii VM (2013) Hydrolysis constants of Al^{3+}, Ga^{3+}, and In^{3+} ions in 0.1 M KNO_3 solution. Russ J Inorg Chem 58:1593-1596
40. Bard AJ, Faulkner LR (1980) Electrochemical methods. Fundamentals and applications. John Wiley & Sons, New York
41. Eigen M, Wilkins RG (1965) The kinetics and mechanisms of formation of metal complexes. Adv Chem 49:55-80
42. Levich VG (1962) Physicochemical hydrodynamics. Prentice Hall, Englewood Cliffs NJ
43. Duval JFL, van Leeuwen HP (2012) Rates of ionic reactions with charged nanoparticles in aqueous media. J Phys Chem A 116:6443-6451
44. Koutecký L, Koryta J (1961) The general theory of polarographic kinetic currents. Electrochim Acta 3:318-339
45. Koryta J, Dvorak J, Kavan L (1993) Principles of electrochemistry. 2nd edn. Wiley, Chichester
46. van Leeuwen HP, Puy J, Galceran J, Cecília J (2002) Evaluation of the Koutecký-Koryta approximation for voltammetric currents generated by metal complex systems with various labilities. J Electroanal Chem 526:10-18
47. van Leeuwen HP, Town RM (2004) Stripping chronopotentiometry at scanned deposition potential (SSCP). Part 4. The kinetic current regime. J Electroanal Chem 561:67-74
48. Town RM, van Leeuwen HP (2004) Dynamic speciation analysis of heterogeneous metal complexes with natural ligands by stripping chronopotentiometry at scanned deposition potential (SSCP). Aust J Chem 57:983-992
49. van Leeuwen HP, Town RM (2006) Stripping chronopotentiometry at scanned deposition potential (SSCP). Part 7. Kinetic currents for ML_2 complexes. J Electroanal Chem 587:148-154
50. van Leeuwen HP, Duval JFL, Pinheiro JP, Blust R, Town RM (2017) Chemodynamics and bioavailability of metal ion complexes with nanoparticles in aqueous media. Environ Sci: Nano 4:2108-2133
51. Heyrovský J, Kuta J (1965) Principles of polarography. Academic Press, New York
52. Zhang Z, Buffle J, van Leeuwen HP (2007) Roles of dynamic metal speciation and membrane permeability in metal flux through lipophilic membranes: general theory and experimental validation with nonlabile complexes. Langmuir 23: 5216-5226
53. Zhang Z, Buffle J (2009) Interfacial metal flux in ligand mixtures, 1. The revisited reaction layer approximation: theory and examples of applications. J Phys Chem A 113:6562-6571
54. van Leeuwen HP (2011) Steady-state DGT fluxes of nanoparticulate metal complexes. Environ Chem 8:525-528

55. Harris WR, Messori L (2002) A comparative study of aluminium(III), gallium(III), indium(III), and thallium(III) binding to human serum transferrin. Coord Chem Rev 228:237-262
56. Brown PL, Ellis J, Sylva RN (1982) The hydrolysis of metal ions. Part 4. Indium(III). J Chem Soc Dalton Trans 1911-1914.
57. Biryuk EA, Nazarenko VA, Ravitskaya RV (1969) Spectrophotometric determination of hydrolysis constants of indium ions. Zh Neorg Khim 14:965-970
58. Tanaka N, Tamamushi R (1964) Kinetic parameters of electrode reactions. Electrochim Acta 9:963-989
59. Rudolph WW, Fischer D, Tomney MR, Pye CC (2004) Indium(III) hydration in aqueous solutions of perchlorate, nitrate and sulfate. Raman and infrared spectroscopic studies and *ab-initio* molecular orbital calculations of indium(III)-water clusters. Phys Chem Chem Phys 6:5145-5155
60. Grahame DC (1947) The electrical double layer and the theory of electrocapillarity. Chem Rev 41:441-501
61. Town RM, van Leeuwen HP (2001) Fundamental features of metal ion determination by stripping chronopotentiometry. J Electroanal Chem 509:58-65
62. van Leeuwen HP, Town RM (2003) Electrochemical metal speciation analysis of chemically heterogeneous samples: the outstanding features of stripping chronopotentiometry at scanned deposition potential. Environ Sci Technol 37:3945-3952
63. Town RM, van Leeuwen HP (2004) Depletive stripping chronopotentiometry: a major step forward in electrochemical stripping techniques for metal ion speciation analysis. Electroanalysis 16:458-471
64. Town RM, van Leeuwen HP (2006) Comparative evaluation of scanned stripping techniques: SSCP *vs*. SSV. Croat Chem.Acta 79:15-25
65. Town RM, van Leeuwen HP (2019) Stripping chronopotentiometry at scanned deposition potential (SSCP): an effective methodology for dynamic speciation analysis of nanoparticulate metal complexes. J Electroanal Chem 853:113530
66. Piercy R (1975) Some aspects of the electrochemistry of indium. PhD Thesis, Loughborough University of Technology, UK
67. Town RM, Pinheiro JP, Domingos R, van Leeuwen HP (2005) Stripping chronopotentiometry at scanned deposition potential (SSCP). Part 6: Features of irreversible complex systems. J Electroanal Chem 580:57-67
68. Niki K, Mizota H (1976) Effect of specific adsorbed anions on the electrode kinetics of the V(III)/V(II) and Eu(III)/Eu(II) couples. J Electroanal Chem 72:307-317
69. van Leeuwen HP, Town RM (2002) Elementary features of depletive stripping chronopotentiometry. J Electroanal Chem 535:1-9
70. DeFord DD, Hume DN (1951) The determination of consecutive formation constants of complex ions from polarographic data. J Am Chem Soc 73:5321-5322